International Conference on Space Optics—ICSO 2006

Noordwijk, Netherlands

27–30 June 2006

Laser interrogation techniques for high-sensitivity strain sensing by fiber-Bragg-grating structures

G. Gagliardi, M. Salza, P. Ferraro, P. De Natale

LASER INTERROGATION TECHNIQUES FOR HIGH-SENSITIVITY STRAIN SENSING BY FIBER-BRAGG-GRATING STRUCTURES

G. Gagliardi, M. Salza, P. Ferraro, and P. De Natale

CNR-Istituto Nazionale di Ottica Applicata and European Laboratory for Non-Linear Spectroscopy, via Campi Flegrei 34, I-80078 Pozzuoli (Naples), Italy

Email: gianluca.gagliardi@inoa.it, mario.salza@inoa.it, pietro.ferraro@inoa.it, paolo.denatale@inoa.it

ABSTRACT

Novel interrogation methods for static and dynamic measurements of mechanical deformations by fiber Bragg-gratings (FBGs) structures are presented. The sensor-reflected radiation gives information on suffered strain, with a sensitivity dependent on the interrogation setup. Different approaches have been carried out, based on laser-frequency modulation techniques and near-IR lasers, to measure strain in single-FBG and in resonant high-reflectivity FBG arrays. In particular, for the fiber resonator, the laser frequency is actively locked to the cavity resonances by the Pound-Drever-Hall technique, thus tracking any frequency change due to deformations. The loop error and correction signals fed back to the laser are used as strain monitor. Sensitivity limits vary between 200 nε/√Hz in the quasi-static domain (0.5÷2 Hz), and between 1 and 4 nε/√Hz in the 0.4-1 kHz range for the single-FBG scheme, while strain down to 50 pε can be detected by using the laser-cavity-locked method.

1. EXPERIMENTAL METHODOLOGY

A sketch of the experimental apparatus is represented in Fig. 1. A 1560-nm DFB diode laser is driven by a Peltier-based PID module and a low-noise power source for temperature control and current supply. The diode is fiber coupled to an array made of two identical FBGs with peak reflectivity > 99.5 % and a relative distance of 13 cm. An external optical isolation stage is used to avoid undesired optical feedback to the laser.
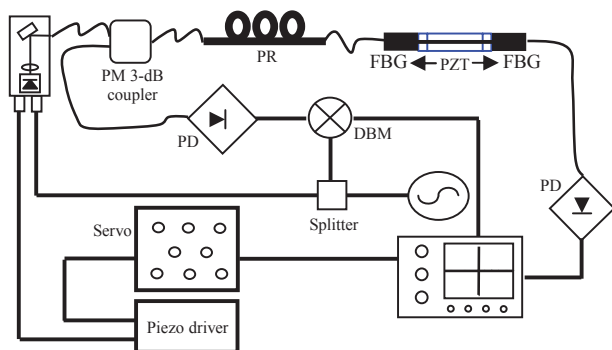

Fig. 1. Cavity-based experimental set-up. PD stands for photodiodes, PR for polarization rotator. The loop error

signal can be visualized on a digital FFT analyzer with a variable bandwidth while it is sent to the servo input for laser frequency corrections.

The FBGs were both protected by small aluminum cylinders in order to keep their Bragg center wavelengths stable. Being the FBGs' center wavelengths substantially coincident, within their spectral width, this structure forms a high-finesse Fabry-Pèrot around 1560 nm with a free-spectral-range (FSR) of approximately 800 MHz. A 50-cm long secondary resonant cavity, fabricated in high-birefringence fiber, is also available for sensing purposes.

The diode-laser frequency is kept tightly locked to the cavity modes by means of an optoelectronic loop, based on Pound-Drever-Hall (PDH) method [13]. The transmission and reflection from the resonator are detected by two pigtailed InGaAs PIN photodiodes. A fiber circulator ensures that the incident and reflected beams are physically separated, while a λ/4-λ/2 rotation stage controls the polarization state of the incident beam. The laser is frequency modulated at about 11 MHz, generating sidebands at this frequency distance from the carrier. Since the leakage field back to the source is basically in antiphase with the input field, the cancellation of these two fields leads to a net reflection coefficient with a strongly frequency-dependent phase shift around the resonance. Hence, the cavity-reflected beam is phase-sensitive demodulated by a double-balanced mixer to generate an even-symmetric, dispersive-like signal that contains information on attenuation and dispersion differences experienced by the sidebands. The cavity transmission maximum exactly corresponds to vanishing of this signal, which is used as error signal of a proportional-integrator (PI) feedback loop for frequency stabilization of the laser to the cavity peaks. In this way, the laser follows any frequency shift of the resonance eventually caused by changes of its optical pathlength. Indeed, thermal and mechanical conditions of the intra-cavity fiber strongly influences the position of its resonances, and thus the error carries information on length variations of the fiber. For this reason, the sensor is also equipped with a passive thermal insulation to maintain its temperature stable during measurements. Strain can be applied to the intra-cavity fiber in a controlled manner by means of a 150-V

piezo-electric transducer acting between the ends of the fiber mount. Its strain response has been accurately calibrated over a wide acoustic-frequency interval via cavity-length modulation using the 11-MHz sidebands as a reference, thus accounting for mechanical coupling and resonances of the PZT with the fiber mount.

2. TEST AND RESULTS

We investigated the strain detection performance of the 13-cm FBG array. In Fig. 2, its transmission, along a wide frequency interval, is shown. For this purpose, the laser diode was frequency-modulated by summing a large triangular-wave signal to the injection current. The graph exhibit a bell-shaped envelope related to the spectral overlap of the two FBGs, where the cavity finesse increases close to the FBG center.
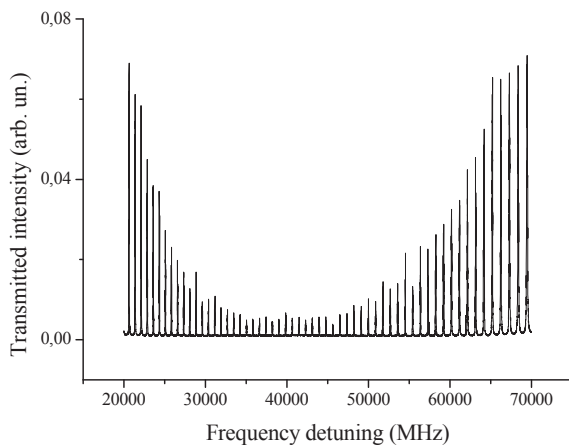

Fig. 2. Transmission of the fiber resonator obtained scanning the laser over a wide spectral bandwidth.

Using the PDH signal derived from the heterodyne detection system described above, the diode laser frequency is maintained locked to one cavity resonance. The circuit corrects laser frequency fluctuations with respect to the cavity, directly acting on the injection current via the driver fast modulation input. Its action has been found to be effective over a time of several hours, in a bandwidth going from DC to about 1 kHz (unity-gain bandwidth). With this in mind, any mechanical or thermal stress applied to the cavity immediately translates to error amplitude changes, thus providing a fast and sensitive strain monitor at frequencies beyond the servo unity-gain. Actually, perturbations acting within the servo bandwidth can be still observed in the PDH signal with a high signal-to-noise ratio because of the imperfect loop correction. In Fig. 3, an example of strain detection with spectral amplitude analysis is shown using the loop error in the

tightly-locked case. In addition, an acoustic wave is excited in the sensing fiber by the PZT. The latter is driven by a 700-Hz ac voltage with a strain-equivalent amplitude of 150 nɛ. Strain calibration can be carried out, as mentioned in the previous section by sweeping the intra-cavity length by about 15 % of the FSR while observing the cavity transmission and using the laser RF sidebands for accurate frequency calibration of the corresponding fiber length variation as a function of the PZT bias voltage and frequency. In Fig. 3, satellite oscillations are still visible from 50 to 350 Hz, regardless of the servo action. These may be consequence of environmental noise that couples to the fiber. An estimate of the signal-to-noise ratio at 700 Hz (40 dB) yields a minimum-detectable strain of about 200 pɛ/√Hz. For operation at frequency higher than the servo unity-gain point, e.g. with a 1.3-kHz signal, we obtained an ultimate limit as low as 20 pɛ/√Hz.
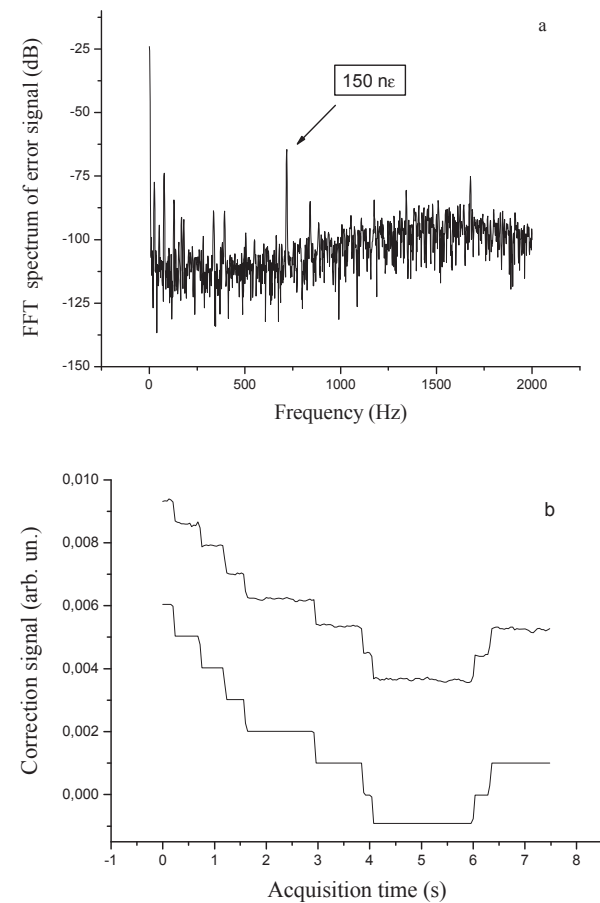

Fig. 3. FFT spectrum of the error signal in the laser-locked condition a) (50-Hz bandwidth). The sharp peak corresponds to a 150-nɛ signal at 700 Hz on the intra-cavity fiber. In graph b), detection of quasi-static strain in the FBG cavity vs. time (8 s), for 600-nɛ steps, is shown.

Nevertheless, the integrated-error signal (i.e. the servo output) fed to the laser for correction, can be used in the low-frequency range as a strain transducer as well. This is particularly relevant when a quasi-static strain monitoring is required. In Fig. 3b, the response of the loop correction signal (namely, the integrated loop output) to step deformations applied by the PZT is shown in the time domain.

A similar detection scheme has been applied to a resonator built by high-birefringence (HiBi) PANDA FBGs, placed at a 50-cm distance. The FBGs have a manufacturer's certified peak reflectivity > 99.5 %. The interrogation system, currently under development, exploits again a cavity-laser lock condition. Some preliminary results are shown in the following. An extended-cavity diode laser, still emitting around a 1560-nm wavelength, is being used for this purpose. The locking technique is basically the same as for the previous set-up. However, the new laser source exhibits a narrower emission spectrum and the cavity-lock action is directed both to the piezo controlling the laser cavity and to the injection current, resulting in a much more efficient stabilization effect. In addition, the coexistence of two different cavity longitudinal modes, corresponding to orthogonal polarizations (SOPs) propagating along the fast and slow fiber axes, is pointed out. In Fig. 4, cavity transmission (with RF sidebands) and PDH signals are shown for both along a single laser sweep. These resonances occur at nearly the same free-spectral-range (about 190 MHz) separated by about 40 MHz, essentially due to the intra-cavity fiber birefringence.
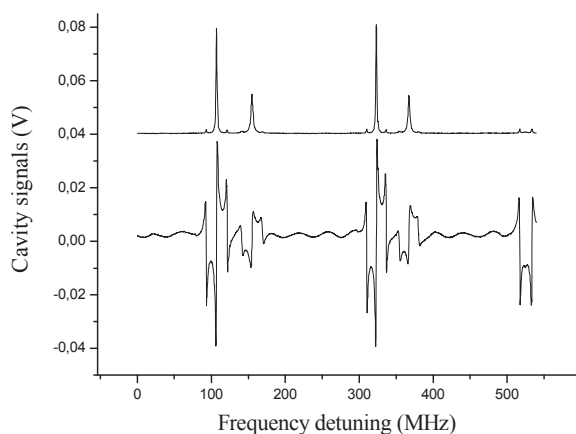
Fig. 4. Transmission and Pound-Drever-Hall error signals recorded for fast and slow axes.

In Fig. 5, detection of a dynamic strain signal (10 nε, 900 Hz) is demonstrated for both SOPs by alternately locking the beam on the two polarization modes. Also in this case, a noise-limited strain sensitivity ranging from 10 to 40 pε/√Hz can be appreciated. The major advantage of this new approach relies in the possibility of using a possible SOP differential response to discriminate between strain and temperature effects contributing to laser-cavity relative frequency shifts.
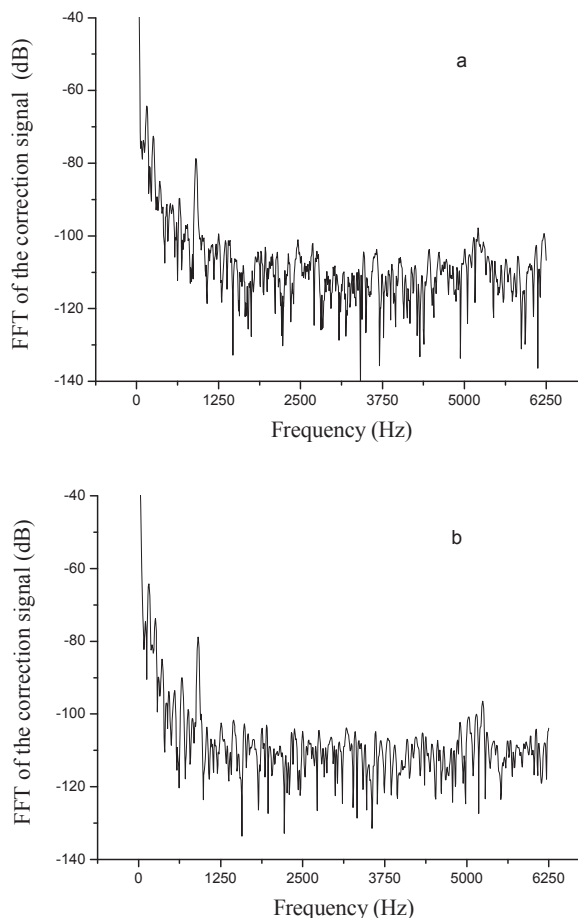
Fig. 5. Dynamic strain response of fast (a) and slow (b) polarization peaks in the laser-cavity locked condition for a 10-ne signal (resolution bandwidth 25 Hz).

As a further improvement, a slightly different interrogation approach, based on polarization-sensitive detection, will be also considered. This scheme promises even better performances in terms of sensitivity and accuracy in strain measurements. In the near future, the polarization-based and the RF stabilization technique will be combined to extend the detection capabilities of HiBi-fiber resonators aimed at simultaneous measurements of strain and temperature by a single sensor.

3. REFERENCES

1. Y.J. Rao, "In-fibre Bragg grating sensors," *Meas. Sci. Technol.* **8** 355 (1997)
2. Y.J. Rao and S. Huang, "Application of Fiber Optic Sensors" in *Fiber Optic Sensors,* F.T.S. Yu and S. Yin

eds., (Marcel Dekker, Inc., New York, 2002) pp. 449-490

3. B. Lee and Y. Jeong, "Interrogation Techniques for Fiber Grating Sensors and the Theory of Fiber Gratings" in *Fiber Optic Sensors*, F.T.S. Yu and S. Yin eds. (Marcel Dekker, Inc., New York, 2002) pp. 295-382

4. L. Crescentini, A. Amoruso, G. Fiocco, G. Visconti, "Installation of a high-sensitivity laser strainmeter in a tunnel in central Italy," *Rev. Sci. Instrum*. **58**, 3206-3210 (1997)

5. P. Ferraro and G. De Natale. "On the possible use of optical fiber Bragg gratings as strain sensors for geodynamical monitoring," *Opt. Laser Eng*. **37**, 115-130 (2002)

6. A. Arie, B. Lissak and M. Tur, "Static Fiber-Bragg Grating Strain Sensing Using Frequency-Locked Lasers," *J. Lightwave Technol.* **17**, 1849-1855 (1999)

7. B. Lissak, A. Arie and M. Tur, "Highly sensitive dynamic strain measurements by locking lasers to fiber Bragg gratings," *Opt. Lett.* **23**, 1930-1932 (1998)

8. G. Gagliardi, M. Salza, P. Ferraro, P. De Natale, "Fiber Bragg-grating strain sensor interrogation using laser radio-frequency modulation," *Opt. Express* **13**, 2377 (2005)

9. C. Wang and S. Scherrer, "Fiber ringdown pressure sensors," Opt. Lett. **29**, 352-354 (2004)

10. P.B. Tarsa, D.M. Brzozoski, P. Rabinowitz, K.K. Lehmann, "Cavity ringdown strain gauge," Opt. Lett. **29**, 1339-1341 (2004)

11. J.H. Chow, D.E. McClelland, M.B. Gray, I.C.M. Littler, "Demonstration of a passive subpicostrain fiber strain sensor,"Opt. Lett. **30**, 1923-1925 (2005)

12. D.W. Kim F. Shen, X. Chen, and A. Wang, "Simultaneous measurement of refractive index and temperature based on a reflection-mode long-period grating and an intrinsic Fabry-Pérot interferometer sensor, " *Opt. Lett.* **30** 3000 (2005)

13. R.W. Drever J.L. Hall, F.V. Kowalski, J. Hough, G.M. Ford, A.J. Munley, H. Ward, "Laser phase and frequency stabilization using an optical resonator," Appl. Phys. B **31,** 97-105 (1983)